Bedforms and Closure Depth on Equilibrium Beaches

by

Douglas L. Inman and Peter N. Adams

Abstract

A closure depth is established from bedform stress relations that determines the seaward extent of equilibrium profiles on beaches. The closure depth becomes a function of sand size and incident wave height that provides the matching conditions for the conjoined shorerise and bar-berm portions of equilibrium profiles defined by the elliptic cycloid solution of Jenkins and Inman (in press). These relations have been coded in the VORTEX mine burial model and field tested (Jenkins et al., in revision). Additional findings from this research are described in our 2002, 2003 and 2004 Annual Reports [Grant Number N00014-02-1-0232, http://www.onr.navy.mil].

Introduction

Closure depth for seasonal beach profiles is usually taken as the depth at which the envelope of profiles converge or close e.g., where the depth change vs depth decreases to a common background error (Figure 1) (e.g., Kraus and Harikai, 1983; Inman et al., 1993). When observations are limited to comparison of two or three surveys, the closure depth becomes that at which the survey lines converge with depth, a point of some uncertainty (e.g., Shepard and Inman, 1951; Nordstrom and Inman, 1973; Birkemeier, 1985). Here we define *closure depth* h_c as the maximum depth at which seasonal changes in beach profile are measurable by field survey, most commonly using fathometers (Inman and Bagnold, 1963).

Because of its importance to the understanding of seasonal changes in beach profiles, closure depth in various terminologies has a much studied history associated with measurements on ocean beaches. Shepard and La Fond (1940) showed that seasonal beach changes began in depths greater than 5 m and extended through the surf zone to the beach face, with the maximum changes occurring between depths of 1.5 m and 3.0 m in the vicinity of the breakpoint-bar. Studies of profile changes show similar winter/summer/winter cyclic changes that are repeated each year on perennial beaches, i.e., those with sufficient sand to form equilibrium summer and winter beach profiles (e.g., Inman et al., 1993; Wright, 1995; Cowell et al., 1999). In general sand from the deeper winter breakpoint-bar is transported onshore during small summer waves, building a steeper beach face with a wide summer berm. Higher waves of winter move sand offshore eroding the summer beach face and forming a gently sloping winter beach out to a deeper breakpoint-bar (Shepard and La Fond, 1940; Shepard, 1950).

The asymptotic nature of the closure of seasonal beach profiles seaward of the surf zone makes an accurate determination of closure depth difficult. Therefore, early on, a three year study was undertaken adjacent to the Scripps Institution of Oceanography at La Jolla California with the dual objectives of obtaining accurate measurements of sand level change in the zone of profile convergence, and of evaluating the accuracy of fathometer surveys of sand level change. A series of five bottom stations were established in water depths of 2.7 m, 6.3 m, 10.0 m, 16.7 m and 22.2 m below MSL, each consisting of an array of six reference rods forced into the bottom, with the protruding portions measured by divers (Inman and

Rusnak, 1956). The two shallow stations were lost during seasonal changes that alternately buried the 2.7 m station while the 6.3 m station rods were lost during a winter cut in sand level that exceeded 61 cm. The three deeper reference rod stations were visited and measured by divers and the stations surveyed by fathometer on a fortnightly to monthly basis during the three year period of 1953-1955 (Table 1). The reference rod study had a standard error in measurement of 1.5 cm, and showed that seasonal sand level changes occurred out to depths of 10 m where the range in level was about 10 cm. The two deeper stations had changes of 5 cm, which were not seasonal in nature, but due to shorter period, unspecified phenomena.

Inman and Bagnold (1963) in their analysis of seasonal sand level changes in the energy profiles of equilibrium beaches, also show the maximum closure depth off Scripps Institution of Oceanography to be about 10 m. They noted that although wave-induced sand motion was observed to occur out to 52 m depth (Inman, 1957), sand motion per se may be associated with phenomena other than the closure depth of seasonal beach profiles.

More recently Hallermeier (1978, 1981) derived a relation for closure depth, by assuming that closure depth is related to sediment suspension energetics given by a critical value of the Froude number,

$$h_c \cong 2.28 H_{ss} - 6.85\left(H_{ss}^2 / gT^2\right) \qquad (1)$$

where H_{ss} is the nearshore storm wave height that is exceeded only 12 hours each year and T is the associated wave period. Hallermeier also defined a deeper depth h_i as the limiting depth for significant on-offshore transport of sand by waves throughout a typical year,

$$h_i = (H_{ss} - 0.3\sigma_{ss})T(g/5000D)^{1/2} \tag{2}$$

where σ_{ss} is the standard deviation of H_{ss} and D is the characteristic grain size, usually from a depth of about 1.5 h_c.

Birkemeier (1985) suggested different values of the constants in equation (1) and found that the simple relation $h_c = 1.57\ H_{ss}$ provided a reasonable fit to his profile measurements at Duck, North Carolina. Cowell et al. (1999) review the Hallermeier relation for closure depth h_c and limiting transport depth h_i and extends the previous data worldwide to include Australia. Their calculations indicate that h_c ranges from 5 m (Point Mugu California) to 12 m (SE Australia), while h_i ranges from 13 m (Netherlands) to 53 m (La Jolla California). They conclude that discrepancies in data and calculation procedures make it "pointless to quibble over accuracy of prediction" in h_c and h_i. In the context of planning for beach nourishment, Dean (2002) observes that "although closure depth.....is more of a concept than a reality, it does provide an essential basis for calculating equilibrated...beach widths."

The Hallermeier relations did not fit our modeling needs (Inman et al., 2005a,b), leading us to seek a closure depth criterion that relates bedform type, sand size and wave height as outlined below.

Bedforms Associated with Equilibrium Beach Profiles

Field studies of bedform and type of sand motion indicate that their relation can be expressed in terms of the wave form of the Shield's stress ratio, $\widetilde{\theta} = \widetilde{\tau} / (\rho_s - \rho) gD$, where the stress $\widetilde{\tau}$ is taken as ρu_{m}^2, ρ_{s} and ρ are the densities of solid grains and water respectively, g is acceleration of gravity, D is median grain diameter, and u_{m} is the near bottom amplitude of the orbital velocity (e.g., Dingler and Inman, 1976; Conley and Inman, 1992). The onset (threshold) of grain motion $\widetilde{\theta}_{\mathrm{t}} = (1.7\,\mathrm{sec}^{-1})T$ is frequency dependent, ranging in value from 8.5 to 34 for wave periods T of 5 s and 20 s respectively,

Vortex ripples.. $\widetilde{\theta}_{\mathrm{t}} \leq \widetilde{\theta} \leq 40$
Transition ripples .... $40 \leq \widetilde{\theta} \leq 240$
Flat bed (carpet flow).. $\widetilde{\theta}_{\mathrm{c}} \geq 240$

The above limits for ripples morphology are graphed in Figure 2, where the critical data from significant waves H_{s} are shown in red to emphasize the governing importance of higher waves in ripple morphology.

Care is to be exercised in the use of H_{rms} vs H_{s} in estimating bedforms from the wave form of the Shields parameter, where the wave stress is assumed to have the form $\widetilde{\tau} = \rho u_{\mathrm{m}}^2$, without the usual ambiguity of a drag coefficient. The mechanics of grain onset $\widetilde{\theta}_{\mathrm{t}}$ and ripple formation and disappearance were originally based on the dynamics of steady state hydraulic flows in laboratories. Dingler and Inman (1976) show that it is the higher groups of ocean waves, represented by H_{s} that are analogous to the steady state laboratory case. In the thermodynamic analysis of Jenkins and

Inman (in press) where H_{rms} is applied to energetics, it is the occasional higher waves represented by H_s that form and modify the ripples. Since $H_s = \sqrt{2} H_{rms}$ and $\tilde{\theta} \sim u_m^2$, there is a factor of 2 difference in the values of $\tilde{\theta}$ calculated from the two wave statistics, but only that from H_s gives a meaningful value of $\tilde{\theta}$. In summary, for any given ocean wave condition, ripple morphology is a function of the significant waves H_s, while the rates of formation and sediment transport are calculated from H_{rms}.

Vortex Ripples

The vortex ripple regime $\tilde{\theta}_t \leq \tilde{\theta} \leq 40$, with a mid range of about $\tilde{\theta} = 25$, implies the existence of a rippled sand bottom, where the groups of high waves cause stresses above the threshold of motion θ_t, but usually below the change to the transition ripple regime. Stresses due to lower waves, between groups, are usually below θ_t. The sand would be motionless until groups of larger waves suspend sand as vortex plumes over the rippled bed. In vortex ripples there is no instantaneous granular exchange from ripple to ripple unless the bottom slope is sufficient to induce a gravitational component of sand motion over a horizontal distance of about $\lambda/2$ or greater. However there could be a net ripple motion associated with differences in on-offshore orbital velocities and/or bed slope (e.g., Inman and Bowen, 1962). Generally, this would be a small slope condition of zero net transport, seaward of the closure depth.

Transition Ripples

The transition ripple regime $40 \le \widetilde{\theta} \le 240$, with a mid range of $\widetilde{\theta} = 140$, indicates a sand bottom of active ripples with changing ripple steepness. Smaller waves between groups of high waves form vortex ripples $(\lambda / \eta \sim 6)$ with distinct vortex plumes above the ripple crests, while groups of higher waves reduce the ripple height, forming transition ripples $(\lambda / \eta \sim 12)$. The vortices associated with transition ripples are intense and remain closer to the lee of the ripple crest. Transition ripples occur in the deeper, seaward portion of the shorerise and may be a common feature in the vicinity of closure depth for equilibrium beaches.

Carpet Flow (flat-bed)

Carpet flow is the most active and intense regime of sand motion under waves and occurs for Shield's numbers above the critical value $\widetilde{\theta}_c = 240$. The bed is flat and wave stresses move sand as sheets or carpets of moving sand that include visually distinct forms referred to as *streaking*, *roiling* and *pluming* (Conley and Inman, 1992). Carpet flow commonly occurs throughout the inner portions of the shorerise and in the vicinity of the breakpoint of waves.

Closure Depth

While it may be reasonable to apply (1) and (2) or its simpler form after Birkemeier (1985), comparisons with the Inman et al. (1993) beach profile data set show that these relations tend to underestimate closure depth. We propose an alternative closure depth relation. This relation is based on two premises: closure depth is the seaward limit of non-zero net transport in the cross-shore direction; and, closure depth is a vortex ripple regime in which no net granular exchange occurs from ripple to ripple. Inman (1957) gives observations of stationary vortex ripples in the field and Dingler and Inman (1976) establish a parametric relationship between dimensions of stationary vortex ripples and the Shield's parameter $\tilde{\Theta}$ in the range $3 < \tilde{\Theta} < 40$. Using the inverse of that parametric relation to solve for the depth gives,

$$h_c = \frac{K_e H_\infty}{\sinh kh_c}\left(\frac{D_o}{D_2}\right)^{\psi} \qquad (3)$$

where K_e and ψ are nondimensional empirical parameters, D_2 is the shorerise median grain size; and D_o is a reference grain size. With $K_e \sim 2.0$, $\psi \sim 0.33$ and $D_o \sim 100\ \mu$m, the empirical closure depths reported in Inman et al. (1993) are reproduced by (3). Figure 3 gives a contour plot calculated from (3) showing the rates at which closure depth increases with increasing wave height and decreasing grain size. Because of the wave number dependence, closure depth also increases with increasing wave period. Figure 3 is based on T = 15 sec., typical of storm induced waves on exposed high-energy coastlines.

Cycloid Theory and Evaluation of Boundary Conditions

Understanding of the foregoing measurements of closure depth can now be placed in the more rigorous framework of theory. Jenkins and Inman (in press) show that shorerise and bar-berm equilibria were found to have an exact general solution belonging to the class of elliptic cycloids that admit to a simple analytic form $h = Ax^m$, where h is depth taken positive downward from mean sea level and x is the cross-shore component, positive in the offshore direction. The elliptic cycloid formulation gives an exact general solution that tells us the nature of the equilibrium beach profile curve and provides valuable guidance to understanding and matching of conjoined curves to empirical boundary conditions. The eccentricity e of the ellipse is the most fundamental variable in the solution. It is governed by the stress nonlinearity of the waves in the shorezone, which in turn is a function of the height and period of waves, the morphology of the inner shelf, and the size of sediment.

The equilibrium profile consists of two conjoined sections, joined at the breakpoint of the waves (Figure 1). The *bar-berm* inner curve extends from the berm crest above the beach face, through the surf zone to the breakpoint-bar; and the *shorerise* outer curve extends from the wave breakpoint seaward to the closure depth. The elliptic cycloid theory shows that both the bar-berm and the shorerise have similar curves, each defined by the trace of the rotating ellipse (Figure 4). The two curves have the same cycloidal form but may differ in detail depending upon the eccentricity e of the ellipse and the boundary conditions.

Before proceeding with the analysis of closure depth it is of interest to consider the larger family of which the elliptic cycloid is a special case. By analogy to the cycloid traced by a point on the surface of a rolling circle, which is a special case of a trochoid, elliptic cycloids are the special case where the cycloid is traced by a point on a rolling ellipse. This family of curves also includes elliptic trochoids traced by points that extend outside of the ellipse on a semimajor or minor axis (prolate elliptic cycloids), as well as on an axis within the ellipse (curtate elliptic cycloids). Out present, first, treatment of theoretical equilibrium beach profiles addresses only the common elliptic cycloid, where the point tracing the cycloidal curve is fixed on the circumference at the end of the semiminor axis (Figure 4). It is to be noted that the slope at the seaward (flat) end of the profile ($\theta = \pi$) is always zero for all members of the elliptic trochoid family of curves. However the profile slope at the landward end ($\theta = 0$) varies with type of elliptic cycloid (prolate/common/curtate). In the future, this refinement could be addressed in conjunction with the slopes of the upper beach face in the bar-berm and the seaward slope from the breakpoint of the shorerise.

In the bar-berm curve, the zero slope in the elliptic cycloid occurs at the breakpoint-bar, at a depth of h_b. However, the zero slope of the shorerise curve at closure depth suggests that this is the depth of water necessary for an equilibrium profile to exist, here called the theoretical closure depth h_c. Along ocean beaches with seaward sloping shelves, the necessary depth always exists but usually with a measurable slope $\beta > 0$.

References

Birkemeier, W. A., 1985, "Field data on seaward limit of profile change," *J. Waterway, Port, Coastal and Ocean Division*, v. III, n. 3, ASCE, p. 598-602.

Conley, D. C. and D. L. Inman, 1992, "Field observations of the fluid-granular boundary layer under near-breaking waves," *Jour. Geophysical Res.*, v. 97, n. C6, p. 9631-9643.

Cowell, P. J., D. J. Hanslow, and J. F. Meleo, 1999, "The shoreface," p. 39-71 in A. D. Short (ed.), *Handbook of Beach and Shoreface Morphodynamics*, John Wiley & Sons, Ltd., New York.

Dean, R. G., 2002, *Beach Nourishment: Theory and Practice*, Advanced Series on Ocean Engineering v. 18, World Scientific, River Edge, NJ, 399 pp.

Dingler, J. R. and D. L. Inman, 1976, "Wave-formed ripples in nearshore sands," p. 2109-2126 in *Proc. 15th Coastal Engineering Conf.*, Amer. Soc. Civil Engin., 3641 pp.

Hallermeier, R. J., 1978, "Uses for a calculated limit depth to beach erosion," *Proc. Coastal Eng. Conf., 16th*, Hamburg, Germany.

Hallermeier, R.J., 1981, "A profile zonation for seasonal sand beaches from wave climate," *Coastal Engineering*, v. 4, p. 253-277.

Inman, D. L., 1957, "Wave-generated ripples in nearshore sands," Technical Memorandum 100, *U. S. Army Corps of Engineers, Beach Erosion Board*, 65 pp.

Inman, D. L., G. A. Rusnak, 1956, "Changes in sand level on the beach and shelf at La Jolla, California," Technical Memorandum 82, *U. S. Army Corps of Engineers, Beach Erosion Board*, 64 pp.

Inman, D. L., and A. J. Bowen, 1962, "Flume experiments on sand transport by waves and currents," *Proc. 8th Conf. Coastal Engineering*, Council on Wave Research, Univ. of Calif., p. 137-150.

Inman, D. L., and R. A. Bagnold, 1963, "Littoral processes," p. 529-553 in M. N. Hill (ed.), *The Sea, vol. 3, The Earth Beneath the Sea*, John Wiley and Sons, NY, London.

Inman, D. L., and S. A. Jenkins, 2002, "Model to Predict Mine Migration and Related Bedform," annual report submitted to ONR Code 322 MG (Tom Drake), 8 pp., 5 figs. http://www.onr.navy.mil

Inman, D. L., and S. A. Jenkins, 2004, "Linked VORTEX Model for Mine Burial Prediction," annual report submitted to ONR Code 321 CG (Tom Drake), 12 pp., 7 figs. http://www.onr.navy.mil

Inman, D. L., and S. A. Jenkins, 2005, "Linked VORTEX Model for Mine Burial Prediction," annual report submitted to ONR Code 321 CG (Tom drake), 6 pp., 3 figs. http://www.onr.navy.mil

Inman, D. L., M. H. S. Elwany, and S. A. Jenkins, 1993, "Shorerise and bar-berm profiles on ocean beaches," *J. Geophys. Res.,* v. 98, n. C10, p. 18181-18199. http://repositories.cdlib.org/sio/cmg/11/

Inman, D. L., P. M. Masters, and S. A. Jenkins, 2005a, "Facing the coastal challenge: modeling coastal erosion in southern California," p. 38-52 in O. T. Magoon et al., (eds.), *California and the World Ocean '02*, Amer. Soc. Civil Eng., Reston, VA, 1431 pp. http://repositories.cdlib.org/sio/cmg/12/

Inman, D. L., S. A. Jenkins, and P. M. Masters, 2005b, "Modeling platforms, terraces, and coastal evolution," p. 647-651 in M. Schwartz (ed.), *Encyclopedia of Coastal Science*, Springer, Dordrecht, Netherlands, 1211 pp. http://repositories.cdlib.org/sio/cmg/7/

Jenkins, S. A., and D. L. Inman, in press, "Thermodynamic solutions for equilibrium beach profiles," *Jour. Geophysical Res.*

Jenkins, S. A., D. L. Inman, M. Richardson, and T. Wever, in revision, "Scour and burial mechanics of objects in the nearshore," *IEEE Jour. Ocean Engineering.*

Kraus, N.C., and S. Harikai, 1983, "Numerical model of the shoreline change at Oanai Beach," *Coastal Engineering*, v. 7, n. 1, p. 1-28.

Nordstrom, C. E., and D. L. Inman, 1973, "Beach and cliff erosion in San Diego County, California," p. 125-131, in A. Ross and R. J. Dowlen (eds.), *Studies on the Geology and Geologic Hazards of the Greater San Diego Area, California*, San Diego Association of Geologists, San Diego, CA.

Shepard, F P., 1950, "Beach cycles in southern California," Technical Memorandum 15, *U. S. Army Corps of Engineers, Beach Erosion Board*, 31 pp.

Shepard, F. P., and E. C. La Fond, 1940, "Sand movements along the Scripps Institution pier," *Amer. Jour. Science*, v. 238, n. 4, p. 272-285.

Shepard, F. P., and D. L. Inman, 1951, "Sand movement on the shallow inter-canyon shelf at La Jolla, California," Technical Memorandum 26, *U. S. Army Corps of Engineers, Beach Erosion Board*, 29 pp.

Wright, L. D., 1995, Morphodynamics of Inner Continental Shelves, CRC Press, Boca Raton, FL, 241 pp.

Table 1. Summary of sand level changes on the beach and shelf at La Jolla, California. [a]

Station Depth ft below [a] MLLW	Station Depth m below [b] MSL	Number of Surveys	Standard Errors of Measurement cm	Range in Mean Sand Level cm	Cyclic Trend
6	2.7				seasonal
18	6.3	11	1.8	> 61	seasonal
30	10.0	45	2.0	9	seasonal
52	16.7	49	1.5	5	yes
70	22.2	40	1.0	5	yes

[a] Source Inman and Rusnak (1956) for three year period 1953-1955.

[b] Station depth in meters relative to mean sea level (MSL), where MSL = MLLW + 0.84 m.

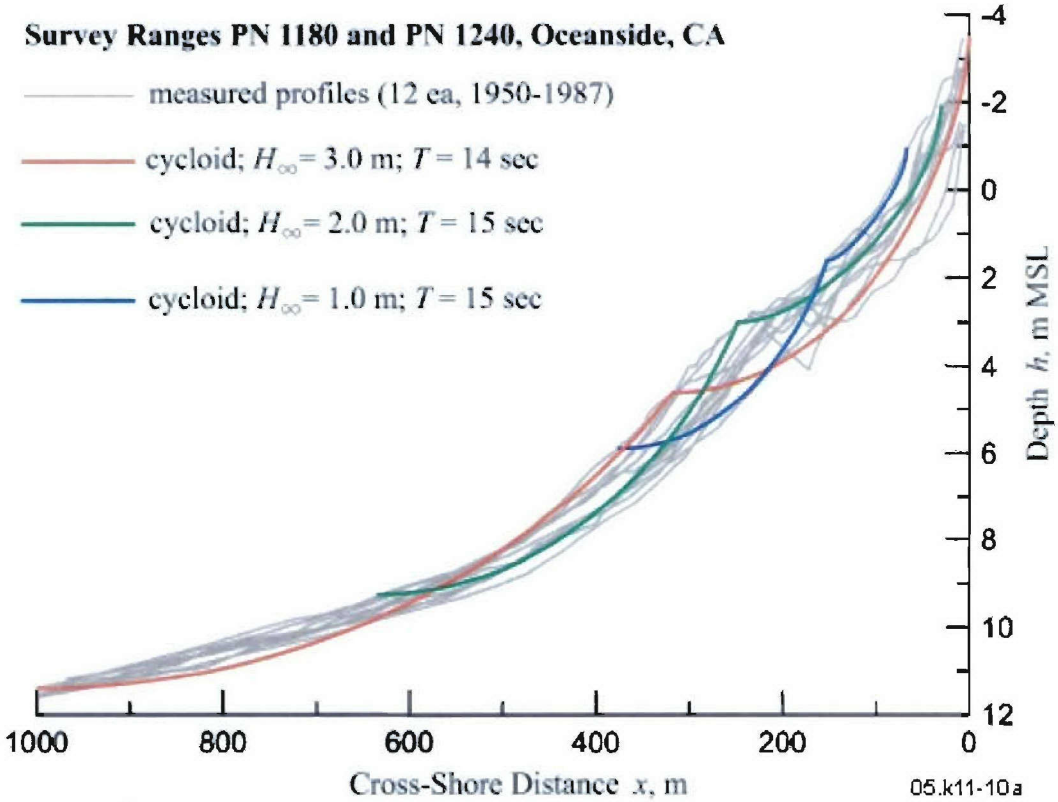

Figure 1. Envelope of variability of 12 measured beach profiles (1950-1987) at Oceanside, CA (gray) compared with the ensemble of type-a elliptic cycloid solutions (colored) for selected incident wave heights and periods with shorerise sand size $D_2 = 100\mu$m and bar-berm sand size $D_1 = 200$ μm. Colored lines break at conjoined point and end at closure depth (from Jenkins and Inman, in press).

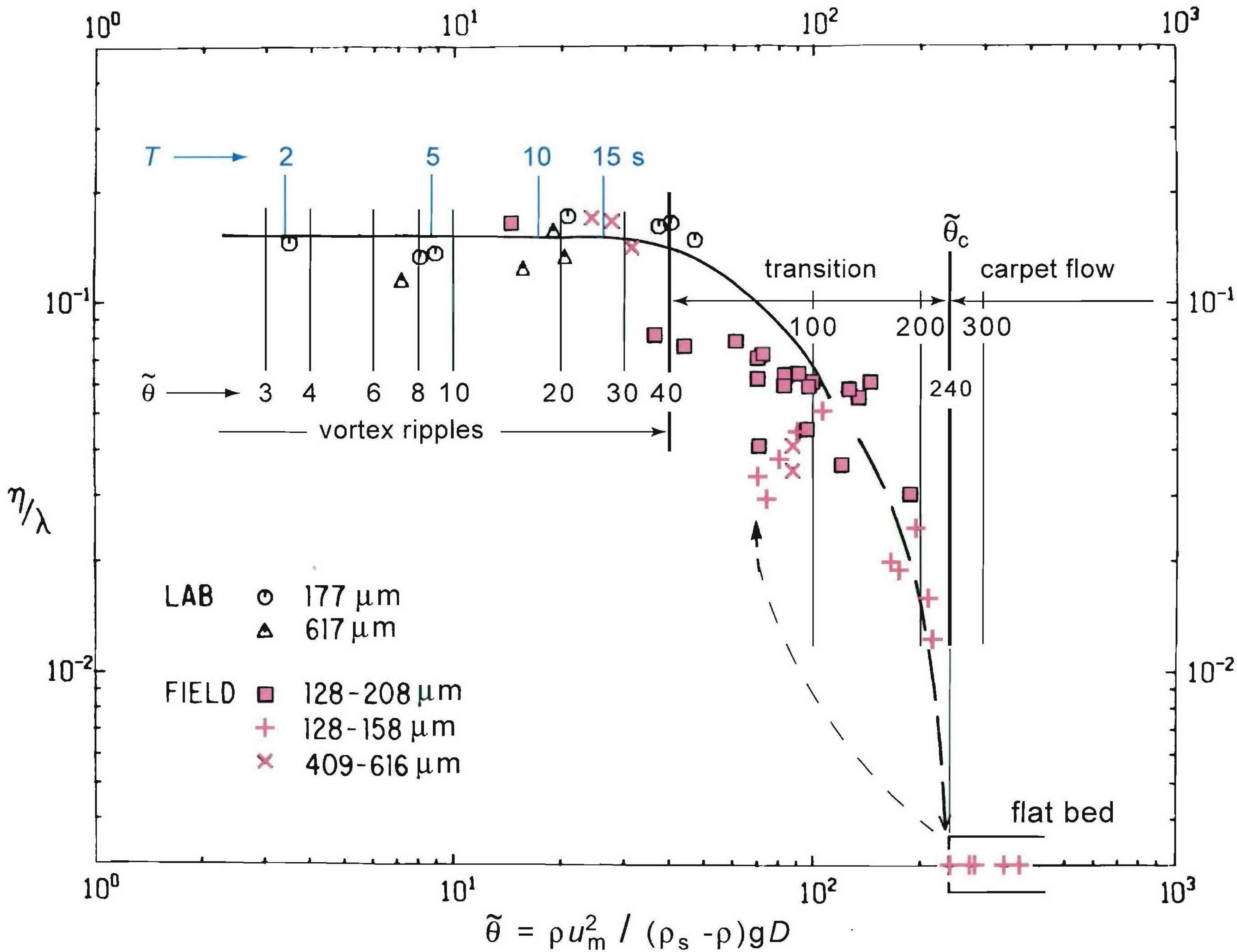

Figure 2. Ripple steepnes η/λ vs relative stress $\tilde{\theta}$ for steady laboratory (○, △) and ocean waves (■, +, ×), the latter computed from significant wave height H_s. Data trends shown as dashed lines; short vertical lines give onset of grain motion $\tilde{\theta}_t$ for selected wave periods T (after Dingler and Inman, 1976).

04.k9e-4a

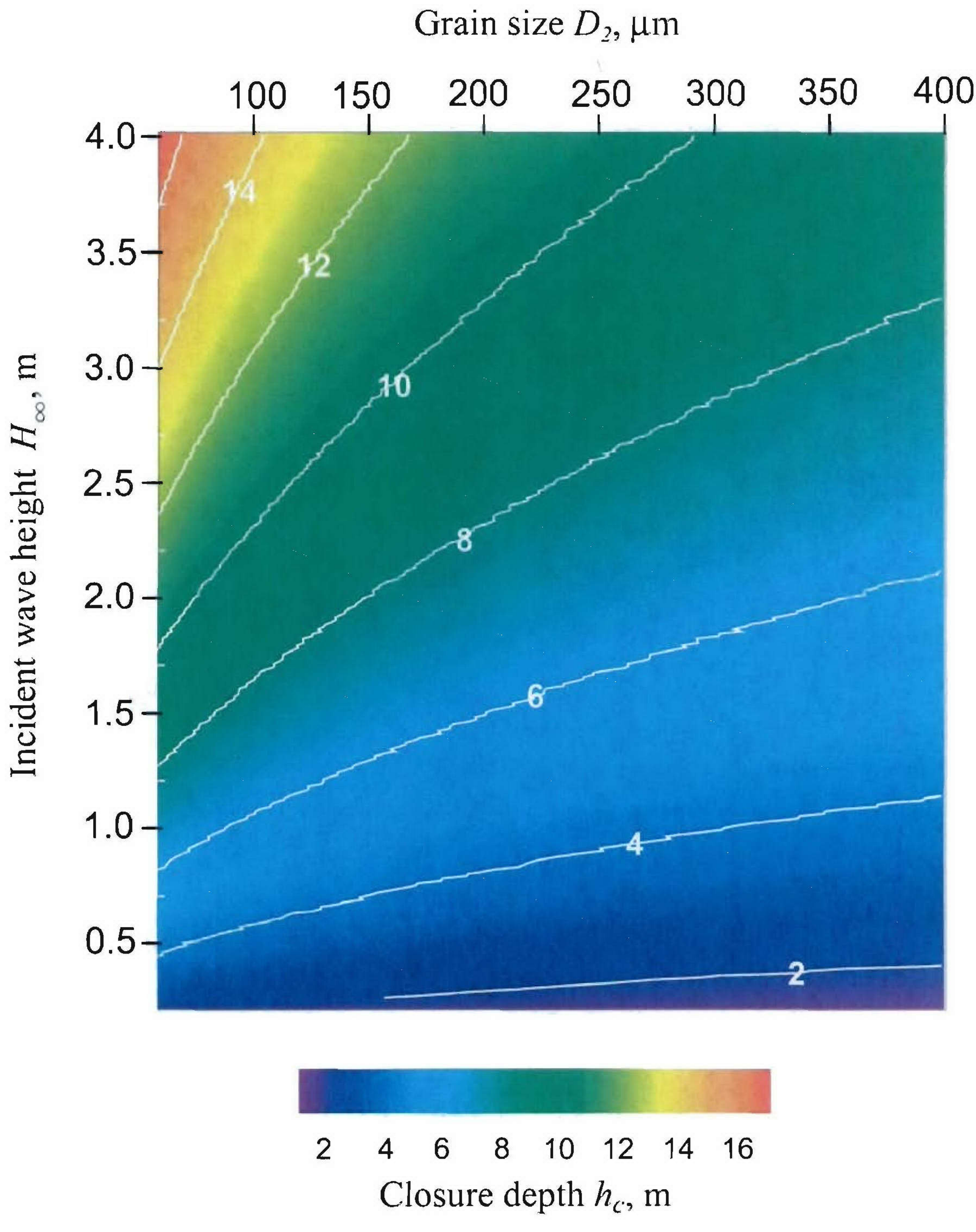

Figure 3. Closure depth h_c from (3) showing dependence on shorerise grain size D_2 and incident wave height H_∞ for waves of 15 sec period ($\psi = 0.33, K_e = 2.0, D_o = 100\mu m$) (from Jenkins and Inman, in press).

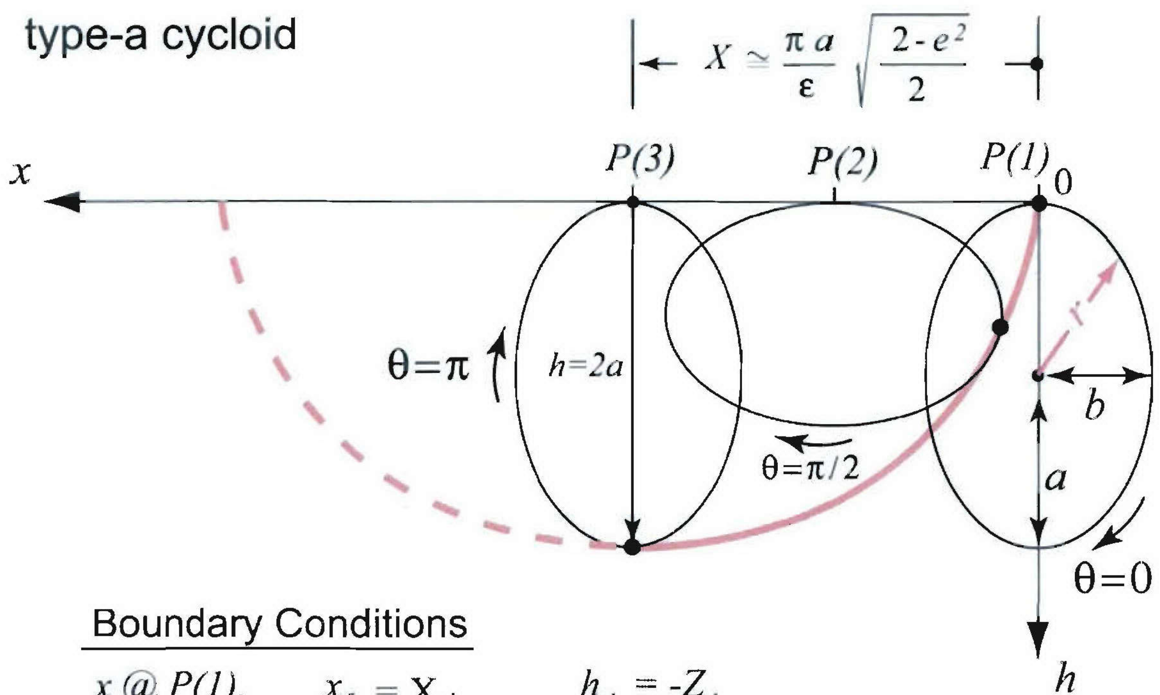

Boundary Conditions

x @ $P(1)$,	$x_1 = X_1$	$h_1 = -Z_1$
$(\theta = 0)$	$x_2 = X_2$	$h_2 = 0$ @ MSL
x @ $P(3)$,	$x_1 = X_3$	$h_1 = h_b$
$(\theta = \pi)$	$x_2 = X_{c2}$	$h_2 = h_c$

05.k11-3a

Figure 4. Elliptic cycloid solution (red line) for the equilibrium beach profile traced by a point on a rolling ellipse with semimajor and semiminor axis a, b, eccentricity $e = \sqrt{1-(b^2/a^2)}$, polar coordinate vector r, angle of rotation θ, and horizontal length scale stretching factor equal 1.0 (from Jenkins and Inman, in press).

REPORT DOCUMENTATION PAGE	Form Approved OMB No. 0704-0188

1. REPORT DATE (DD-MM-YYYY)	2. REPORT TYPE	3. DATES COVERED (FROM - TO)
31-12-2005	Final Technical Report	01-JAN-2002 - 31 DEC 2005

4. TITLE AND SUBTITLE
Model to Predict Mine Migration and Related Bedform

5a. CONTRACT NUMBER

5b. GRANT NUMBER
N00014-02-1-0232

5c. PROGRAM ELEMENT NUMBER

6. AUTHOR(S)
Douglas L. Inman and Peter N. Adams

5d. PROJECT NUMBER

5e. TASK NUMBER

5F. WORK UNIT NUMBER

7. PERFORMING ORGANIZATION NAMES(S) AND ADDRESS(ES)
Scripps Institution of Oceanography
Integrative Oceanography Division
9500 Gilman Drive
La Jolla, CA 92093-0209

8. PERFORMING ORGANIZATION REPORT NUMBER

9. SPONSORING/MONITORING AGENCY NAME(S) AND ADDRESS(ES)
Office of Naval Research
Attn: Dr. Brian Almquist, Code 321 CG
875 North Randolph Street
Arlington, VA 22203-1995

10. SPONSOR/MONITOR'S ACRONYM(S)
ONR

11. SPONSORING/MONITORING AGENCY REPORT NUMBER

12. DISTRIBUTION AVAILABILITY STATEMENT
APPROVED FOR PUBLIC RELEASE

13. SUPPLEMENTARY NOTES

14. ABSTRACT
Bedforms establish a closure depth that determines the seaward extent of mine burial and exposure associated with changes in beach profiles. These relations have been coded in the VORTEX mine burial model and field tested (Jenkins and Inman, in press; Jenkins et al., in revision). Additional findings from this research are described in our 2002, 2003 and 2004 Annual Reports [Grant Number N00014-02-1-0232, http://www.onr.navy.mil].

15. SUBJECT TERMS
bedfroms; beach profile; closure depth; elliptic cycloid; mine burial; sand size; Shield's stress; wave height; vortex ripples

16. SECURITY CLASSIFICATION OF: a. REPORT	b. ABSTRACT	c. THIS PAGE	17. LIMITATION OF ABSTRACT	18. NUMBER OF PAGES	19a. NAME OF RESPONSIBLE PERSON / 19b. TELEPHONE NUMBER (Include area code)
Unrestricted	Unrestricted	Unrestricted	None		Douglas L. Inman / 858-534-4334

Standard Form 298 (Rev. 8-98)
Prescribed by ANSI-Std Z39-18